

High-quality-factor and small-mode-volume hexapole modes in photonic-crystal-slab nanocavities

Han-Youl Ryu^{a)} and Masaya Notomi

NTT Basic Research Laboratories, 3-1 Morinosato-Wakamiya, Atsugi 243-0198, Japan

Yong-Hee Lee

Department of Physics, Korea Advanced Institute of Science and Technology, Taejeon 305-701, Korea

(Received 10 July 2003; accepted 19 September 2003)

Using finite-difference time-domain calculations, we investigate the hexapole mode of photonic-crystal-slab modified triangular single-defect cavity structures as a good candidate for a high-quality factor (Q) and small-mode volume (V) resonant mode. Structural parameters are optimized to obtain very large Q of even higher than 2×10^6 with small effective V of the order of cubic wavelength in material, the record value of theoretical Q/V . It is found, by the Fourier-space investigation of resonant modes, that such a high Q from the hexapole mode is achieved due both to the cancellation mechanism related to hexagonally symmetric whispering-gallery-mode distribution and to the mode delocalization mechanism. © 2003 American Institute of Physics. [DOI: 10.1063/1.1629140]

Microcavity resonant modes with a high quality factor (Q) and small mode volume (V) can potentially be used for miniaturized photonic devices, such as low-threshold lasers,¹⁻⁵ channel drop filters,^{6,7} and nonlinear elements.⁸ In addition, high- Q and small- V modes have attracted growing interest in quantum optical devices of controlled single-photon sources and entangled emitter-cavity system.⁹⁻¹¹ Photonic crystal slab (PCS) defect cavities that can create high- Q resonant modes with wavelength-sized small V are expected to be excellent cavity structures for such purposes. Several groups have reported the design of high- Q PCS cavities for $Q > 10^4$ together with effective V of the order of the cubic wavelength in material $[(\lambda/n)^3]$.¹²⁻¹⁶

Recently, one of the authors has introduced a high- Q resonant mode in a square lattice single-defect cavity.^{13,15} It has been argued that properties of this mode are similar to those of the lowest-order whispering gallery mode (WGM), and the WGM-like field distribution results in a high vertical Q approaching 10^5 . In some applications, however, this mode would not be attractive since bandgap size of the square lattice is much smaller compared to that of the triangular lattice. In this letter, we study the hexapole mode formed in a triangular lattice modified single-defect cavity as a good candidate for a high- Q and small- V resonant mode. This mode has properties of the WGM, with an azimuthal mode number of 3. Considering that out-of-plane radiation angle decreases as the mode number increases in WGMs,² we expect the hexapole mode will show higher Q than the square lattice WGM.

Electric field intensity distribution of the hexapole mode is shown in Fig. 1(a). Here, central defect geometry is modified so that donor-type modes can be pulled down from the air band edge.¹⁷ As shown in Fig. 1(b), six nearest-neighbor holes around the defect cavity are reduced in size and pushed away from the center. The hexapole mode exhibits a standing

wave pattern along the cavity boundary and null electromagnetic energy at the center. This mode pattern is reminiscent of the WGM in a microdisk cavity. However, the hexapole mode is a nondegenerate single mode, unlike the microdisk WGM.

Resonant frequencies, Q , and V are calculated using the finite-difference time-domain (FDTD) method with the perfectly matched layer boundary condition. In the calculation, we vary the radius of regular holes (r) and modified nearest-neighbor holes (r_m) to optimize the Q and the V . Thickness of the air-bridge slab is fixed to $0.6a$, where a is lattice constant, and the refractive index of a slab material is assumed to be 3.4. The vertical Q is evaluated from total energy decay and extraction efficiency. The position that separates the vertical radiation from the in-plane loss is chosen to be $0.5a$ from the slab surface. We consider sufficiently large calculation domains so that the total Q can be larger than half of the vertical Q in order to minimize evaluation uncertainty of the vertical Q . The effective V for the cavity quantum electrodynamics (CQED) is defined as the ratio of total electric field energy to the maximum of the electric field energy density.¹²

In Fig. 2, vertical Q and effective V are plotted as a function of resonant frequencies for some values of r_m when r is $0.35a$. Dotted lines indicate band-edge frequency positions. The largest vertical $Q \sim 5 \times 10^5$ is obtained when r_m is $0.26a$. We confirm that the total Q approaches the vertical Q when the structure size is $\sim (15a)^2$. This is much larger than vertical Q reported in previous works.¹²⁻¹⁶ In this case, small effective $V < 0.9(\lambda/n)^3$ is also obtained because the resonant mode is well confined inside the bandgap. Still, large vertical $Q > 10^4$ are observed in a wide range of r_m values deviated from $0.26a$. The achievement of such high Q from the hexapole mode is attributed to hexagonally symmetric WGM-like field distribution. Since the phases of adjacent lobes are opposite to each other, destructive interference is expected in the vertically radiating field. This is basically related to the

^{a)}Electronic mail: hyryu@will.brl.ntt.co.jp

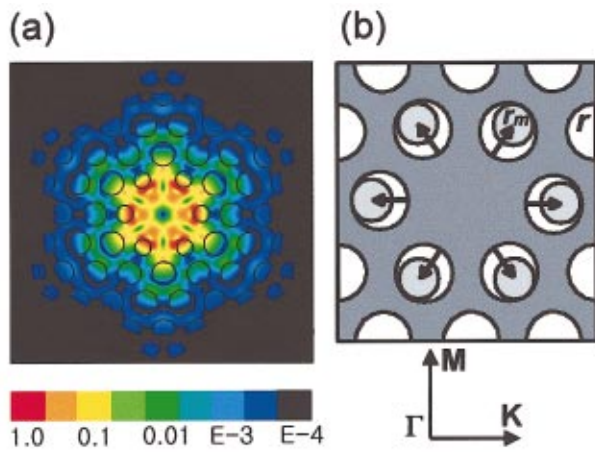


FIG. 1. (Color) (a) Electric field intensity distribution of the hexapole mode in a triangular lattice modified single-defect cavity. (b) Modified single-defect cavity. Six nearest-neighbor holes are pushed away from the center. r and r_m denote the radius of regular holes and modified nearest-neighbor holes, respectively.

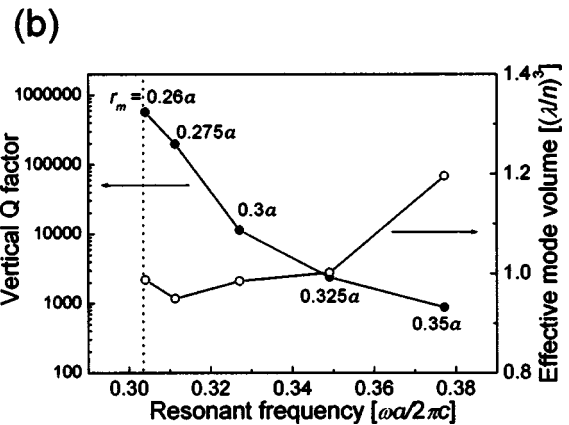
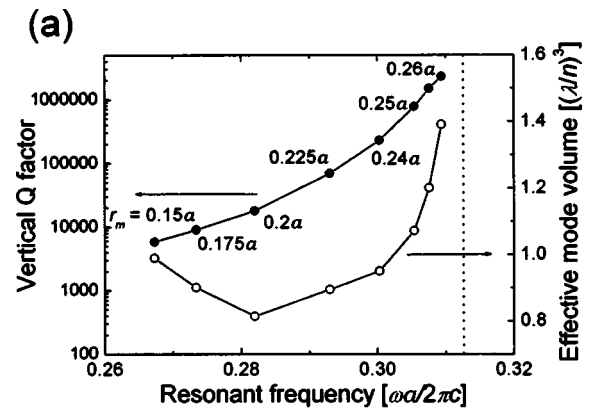


FIG. 3. Vertical Q and effective V as a function of resonant frequencies. Solid and open circles represent vertical Q and effective V , respectively. (a) r is $0.275a$. Dotted line indicates the air band-edge position. (b) r is $0.4a$. Dotted line indicates the dielectric band edge position.

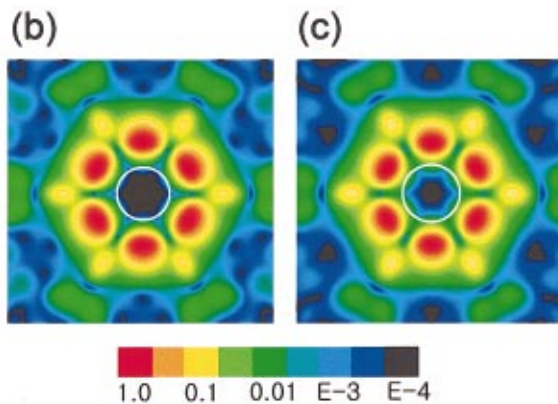
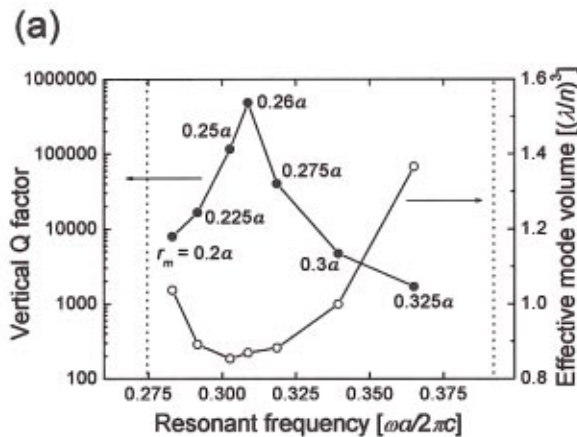


FIG. 2. (Color) (a) Vertical Q and effective V as a function of resonant frequencies for some values of r_m when r is $0.35a$. Solid and open circles represent vertical Q and effective V , respectively. Dotted lines indicate band-edge frequency positions. (b) Fourier- k -space electric field intensity when r_m is $0.26a$. A solid circle represents the light cone boundary. Here, the vertical Q is 480 000. (c) Fourier- k -space electric field intensity when r_m is $0.3a$. The vertical Q is 11 000.

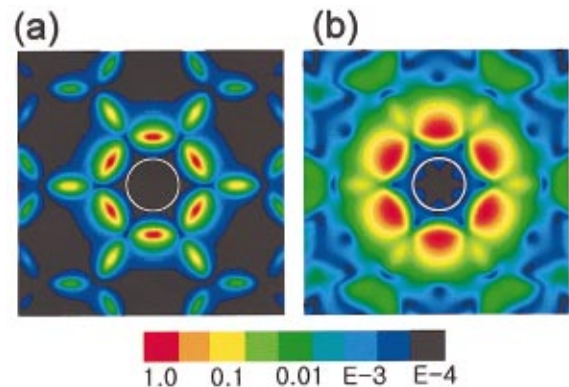


FIG. 4. (Color) Fourier-space electric field intensity. (a) r is $0.275a$ and r_m is $0.26a$. The vertical Q is 2 300 000. (b) r is $0.4a$ and r_m is $0.26a$. The vertical Q is 570 000.

which results in a high vertical $Q \sim 5 \times 10^5$. The weak intensity near the light cone center can be viewed as the contribution of the cancellation mechanism, and the weak intensity region will be broader as the cancellation mechanism works better as in Fig. 2(b).

In Fig. 3, vertical Q and effective V are plotted when r is $0.275a$ and $0.4a$. Here, resonant frequencies for maximum vertical Q are positioned near the air band edge and the dielectric band edge, respectively. It is interesting to note that the largest vertical Q are again achieved when r_m is $0.26a$ for both cases. This implies that the cancellation mechanism works very well for the mode distribution when r_m is near $0.26a$, regardless of r values. Actually, main features of mode profiles are determined by the r_m because the fields are mostly distributed around the nearest-neighbor holes. In Fig. 3(a), the largest vertical Q is even higher than 2×10^6 ; that is, more than one order of magnitude larger than previous results on high- Q photonic crystal cavity modes.^{12–16} In this case, V is somewhat increased to $\sim 1.4(\lambda/n)^3$. Therefore, a mode delocalization mechanism^{18,20} is believed to contribute to such a high vertical Q . We again confirm that the total Q approaches the vertical Q in a large calculation domain. In this case, very large structure size $\sim (45a)^2$ is needed to get the total $Q > 2 \times 10^6$ due to the strong delocalization effect. When r is $0.4a$ and r_m is $0.26a$, however, the vertical Q is $< 6 \times 10^5$ and effective V is still less than $(\lambda/n)^3$. Thus, the delocalization mechanism is not so much responsible for the high Q in this case, although the resonant mode exists just above the dielectric band edge.

Fourier-space mode patterns corresponding to above results are shown in Fig. 4. When r is $0.275a$ and r_m is $0.26a$, the size of dominant k components region near six M points is much reduced. This is a direct consequence of the mode delocalization since the resonant frequency is near the band edge positioned at the M point. Due to this effect, k -space field intensity near the light cone boundary is much reduced, which partly contributes to the high vertical Q . That is, low intensity near the light cone periphery and near the central region is attributed to the delocalization mechanism and the cancellation mechanism, respectively. Due to these combined effects, intensity in all regions inside the light cone is lower than 10^{-4} of peak intensity, and thus the extremely high vertical $Q > 2 \times 10^6$ is achieved. When r is $0.4a$ and r_m is $0.26a$, however, the size of dominant k components is still large. This is because the resonant mode exists near the dielectric band edge at the K point that is far from the dominant k components of the hexapole mode. Therefore, the delocalization mechanism is not so effective in this case and the vertical Q is limited below 10^6 .

When r is $0.275a$ and r_m is $0.26a$, the Purcell factor⁹ is evaluated to be larger than 10^5 . This is an extremely high theoretical value for all types of resonant modes. In fact, a very high $Q > 10^8$ has recently been demonstrated experimentally from the toroidal microcavity with diameter of $\sim 100 \mu\text{m}$.²¹ In this cavity mode, the Purcell factor based on experiments is estimated to be $\sim 10^4$. However, such high Purcell effects might not be achieved in real experiments in this high- Q and small- V mode because strong interaction between the emitter and the cavity mode may give rise to Rabi oscillations, a strong coupling regime of the CQED.¹⁶

Now, we would like to mention the potential importance of very high vertical- Q resonant modes in PCS structures. They can be used for in-plane routing of emission with high outcoupling efficiency since out-of-plane optical loss is negligibly small. For example, let us consider photon extraction from the cavity mode with a vertical Q of 10^6 via a PC waveguide with a coupling Q of 10^4 . In this case, one can achieve very high collection efficiency $\sim 99\%$ in principle, while preserving a high- Q ($\sim 10^4$) system. In fact, most PCS cavities have utilized vertical emission for lasers^{4,5} and filters.⁷ The maximum collection efficiency of these vertical emitting devices is 50% at best since downward photons are not collected normally. In this sense, the high vertical- Q hexapole mode is quite promising for a low-loss photonic integrated circuit element and high collection-efficiency single-photon sources for quantum cryptography.

In conclusion, we have numerically demonstrated very high- Q and small- V resonance from the hexapole mode of the triangular lattice modified single-defect cavity. High $Q > 2 \times 10^6$ and small mode volume $\sim (\lambda/n)^3$ are obtainable by optimization of structural parameters based on the FDTD calculation. Hence, the very high value of a theoretical Purcell factor $> 10^5$ is obtained from the hexapole mode. The mechanisms for high Q are exploited using Fourier space analyses, and it is found that both the cancellation and the delocalization mechanism contribute to the achievement of such high Q . We expect the hexapole mode is well suited to realize high-outcoupling-efficiency planar photonic circuits and single-photon sources.

¹H. Yokoyama, *Science* **256**, 66 (1992).

²R. E. Slusher, A. F. J. Levi, U. Mohideen, S. L. McCall, S. J. Pearton, and R. A. Logan, *Appl. Phys. Lett.* **63**, 1310 (1993).

³T. Baba, *IEEE J. Sel. Top. Quantum Electron.* **3**, 808 (1997).

⁴O. Painter, R. K. Lee, A. Scherer, A. Yariv, J. D. O'Brien, P. D. Dapkus, and I. Kim, *Science* **284**, 1819 (1999).

⁵H. Y. Ryu, H. G. Park, and Y. H. Lee, *IEEE J. Sel. Top. Quantum Electron.* **8**, 891 (2002).

⁶S. Fan, P. R. Villeneuve, J. D. Joannopoulos, and H. A. Haus, *Phys. Rev. Lett.* **80**, 960 (1998).

⁷S. Noda, A. Chutinan, and M. Imada, *Nature (London)* **407**, 608 (2000).

⁸S. M. Spillane, T. J. Kippenberg, and K. J. Vahala, *Nature (London)* **415**, 621 (2002).

⁹J. Gérard and B. Gayral, *Physica E (Amsterdam)* **9**, 131 (2001).

¹⁰P. Michler, A. Kiraz, C. Becher, W. V. Schoenfeld, P. M. Petroff, L. Zhang, E. Hu, and A. Imamoglu, *Science* **290**, 2282 (2000).

¹¹C. Santori, D. Fattari, J. Vučković, G. S. Solomon, and Y. Yamamoto, *Nature (London)* **419**, 594 (2002).

¹²J. Vučković, M. Lončar, H. Mabuchi, and A. Scherer, *Phys. Rev. E* **65**, 016608 (2001).

¹³H. Y. Ryu, S. H. Kim, H. G. Park, J. K. Hwang, Y. H. Lee, and J. S. Kim, *Appl. Phys. Lett.* **80**, 3883 (2002).

¹⁴K. Srinivasan and O. Painter, *Opt. Express* **10**, 670 (2002).

¹⁵H. Y. Ryu, J. K. Hwang, and Y. H. Lee, *IEEE J. Quantum Electron.* **39**, 314 (2003).

¹⁶J. Vučković and Y. Yamamoto, *Appl. Phys. Lett.* **82**, 2374 (2003).

¹⁷H. G. Park, J. K. Hwang, J. Huh, H. Y. Ryu, S. H. Kim, J. S. Kim, and Y. H. Lee, *IEEE J. Quantum Electron.* **38**, 1353 (2002).

¹⁸S. G. Johnson, S. Fan, A. Mekis, and J. D. Joannopoulos, *Appl. Phys. Lett.* **78**, 3388 (2001).

¹⁹J. Vučković, M. Lončar, H. Mabuchi, and A. Scherer, *IEEE J. Quantum Electron.* **38**, 850 (2002).

²⁰P. R. Villeneuve, S. Fan, S. G. Johnson, and J. D. Joannopoulos, *IEEE Proc.: Optoelectron.* **145**, 384 (1998).

²¹D. K. Armani, T. J. Kippenberg, S. M. Spillane, and K. J. Vahala, *Nature (London)* **421**, 925 (2003).